METAMORPHISM AND SKARN MINERALISATION IN THE COBAR BASIN: IMPLICATIONS FOR EXPLORATION

J.A. Fitzherbert*
Geological Survey of New South Wales
Department of Planning & Environment
Maitland, New South Wales, 2330
joel.fitzherbert@industry.nsw.gov.au

P.L. Blevin
Geological Survey of New South Wales
Department of Planning & Environment
Maitland, New South Wales, 2330
phil.blevin@industry.nsw.gov.au

A.R. McKinnon
Aurelia Metals Limited
Orange, New South Wales, 2800
adam.mckinnon@aureliametals.com.au

SUMMARY

A metamorphic map of the Siluro-Devonian Cobar Basin highlights zones of high heat (hornblende hornfels facies) overprinting cool (sub-greenschist facies) southern basin sequences. Contrary to current models for mineralisation in the Cobar Basin, which involve metals/fluids derived from basement during regional metamorphism and basin inversion, these zones of localised, large thermal contrast imply proximal, albeit blind, magmatic heat sources. Mineralisation in the main northern Cobar mineral field is associated with greenschist facies high-strain zones and is linked with fluids that exploited major fault systems and regional lithological contacts. Correlative mineralisation along these same fault systems and lithological contacts at Hera and Nymagee orebodies to the south, is associated with hornblende hornfels facies skarn alteration and Au–Ag–Cu–Zn–Pb mineralisation. Petrographic studies at Hera reveal orebody-scale mineralogical zonation from southern garnet-rich, central pyroxene-rich and northern anorthite–tremolite-rich skarn (with remnant carbonate blocks/clasts). Chemical composition of skarn minerals, including sub-calcic garnet (Mn–Ca-rich), low-Mo scheelite, Mn-enriched diopside/tremolite, zoisite and anorthite are consistent with the Hera–Nymagee orebodies representing reduced, low XCO_2 distal Zn(W–Cu–Au)-skarns. Stable isotope (H–O–S) data from the Hera and Nymagee orebodies are consistent with magmatic water/sulfur sources, with formational water/sulfur also represented. A distal skarn origin for mineralisation in the southeastern Cobar Basin and the distinction of zones of elevated hydrothermal heat reflect a relatively intrusion proximal southern mineral system, while correlative deposits in the main Cobar mineral field to the north are hosted in lower temperature hydrothermal zones and likely reflect relatively intrusion-distal parts of the same magmatically driven system. Zn-rich skarns akin to the Hera–Nymagee orebodies generally occur in the distal portions of major magmatic/hydrothermal systems. Thus, the absence of near-orebody intrusions implies the mineral systems of the southeastern Cobar Basin may not have been traced to their ends and the basin is immature with respect to exploration for skarn and intrusion-related mineral systems.

Key words: Cobar Basin, Hera–Nymagee, metamorphism, skarn

INTRODUCTION

The c.420 Ma Cobar Basin is a major mining province in central New South Wales, with an estimated metal endowment exceeding 134.9 t Au, 1.91 Mt Cu, 3.46 Mt Zn, 1.8 Mt Pb and 3832 t Ag. The basin sequences were deposited over Ordovician basement during the Siluro-Devonian. Deep-water parts of the basin interfinger (now mostly fault-bound) with two volcanogenic troughs to the south (Rast Trough) and west (Mount Hope Trough), and are flanked by limestone-bearing shelf sequences to the east (Kopyje Shelf) and west (Winduck Shelf). The eastern shelf reflects an early rift, subsequently drowned shelf sequence and also hosts a number of syn-rift volcanic sequences (Mineral Hill–Canbelego volcanic belt; Figure 1a). The lower stratigraphic levels of the southeastern deep-water basin, shelf sequences and Ordovician basement are intruded by syn-rift I-type plutons along the southeast margin of the basin and eastern shelf sequences (Figure 1a), while volcanogenic sequences of the Mount Hope Trough, and parts of the interfingering siliciclastic basin to the north, are intruded by A, I and S-type intrusive rocks.

The Cobar Basin was inverted and deformed between 405 and 380 Ma (Perkins et al. 1994; Glen et al 1992, 1996). Basin inversion was associated with reactivation of major, basin axial or near margin faults. Cobar-type Cu–Au (Pb–Zn–Ag) deposits occur in a belt along the eastern margin of the Cobar Basin (Figure 1a). Mineralisation is mostly associated with zones of faulting, shear zone development and greenschist facies hydrous metamorphism, although the effects of deformation are diminished to the south and the grade of localised hydrous metamorphism increases to hornblende hornfels facies. The eastern Cobar type deposits have been variously classified as reactivated/remobilised syndepositional subhalative/exhalative (Suppel 1984), epithermal and volcanogenic massive sulfide deposits (David 2006), but a structurally controlled mineral system model with metals derived from metamorphism of basement and basin has remained in vogue throughout the years (e.g. Lawrie & Hinman 1998; Stegman 2001). Despite this, a magmatic character to metal-bearing fluids has been suggested (e.g. Cleverley & Barnicoat 2007; Berthelsen 2010).

A comprehensive metamorphic map of the Cobar basin was constructed by Fitzherbert et al. (2017) and is updated here in Figure 1b. The metamorphic map was constructed primarily through new petrographic observation, historic petrographic re-evaluation (GSNSW petrographic collection) and new determinations of conodont alteration indices (CAI) from shelf limestones and allochthonous limestone blocks within the deeper-water basin sequences. The map also relies heavily on published geothermometry, including, but not exclusive to, mica crystallinity, chlorite thermometry, fluid inclusion trapping temperatures and vitrinite reflectance reported from samples both proximal and distal to mineralisation. See Fitzherbert et al.(2017a) for a detailed account of map construction and data sources, but the most important feature of the metamorphic map for this study is the recognition of two

zones of elevated hydrothermal metamorphism/alteration (hornblende hornfels facies) along the margins of the preserved deep-water parts of the southern basin (Figure 1b).

Deposits/prospects classified as Cobar-type on the southeastern margin of the basin are hosted within siliciclastic-dominant turbidite sequences of the lower Amphitheatre Group and to a lesser extent early-rift siliciclastic to shelf carbonate-bearing sequences of the Mouramba Group (Figure 1a). Mineralisation in the form of massive sulfide breccia and vein systems is associated with calc-silicate to calc-potassic skarn alteration. Petrographic and mineral chemical characteristics (electron microprobe analysis) of the alteration reveal a reduced calcic-Zn(Au–W) skarn at Hera and spatially separated reduced calcic Zn and aluminous Fe-rich, Cu skarn at Nymagee orebody, while low molybdenum contents of scheelite (deep blue florescence under short wavelength UV light) is also consistent with a reduced-skarn origin. Stable isotope (H–O–S) data from the Hera–Nymagee orebodies are consistent with a magmatic fluid and sulfur source, with formational water and sulfur also represented in the data.

The deposits are spatially associated with a major basin margin fault, the Rookery Fault. However the orebodies are located west of this fault system within a sequence dominated by fine-grained basin sequences, but locally rich in sandstone, gritstone and allochthonous carbonate blocks (now skarn). Interestingly, similar allochthonous packages occur at equivalent and higher stratigraphic levels (Shume Formation) at a number of locations throughout the basin, associated with lower temperature mineralisation (e.g. Mallee Bull; Brown et al. 2015). High temperature skarn mineralisation is also present within these higher-level allochthonous packages (Shume Formation) at the Norma Vale prospect north of the Mount Hope Trough (Fitzherbert et al. 2017).

METAMORPHISM IN THE COBAR BASIN

Fitzherbert et al. (2017) describe the distribution of metamorphic grade in the Cobar Basin (updated map Figure 1b). The map can be summarised as:
Western shelf sequences
- Late diagenetic zone burial metamorphism
Eastern early-rift, drowned shelf and volcanic belt
- Predominantly low-anchizone burial and zeolite facies ocean-floor metamorphism in the north
- Biotite-zone greenschist hydrothermal/contact metamorphism in the southwest
- Late diagenesis in the south east with local lower greenschist facies thermal perturbation
- Thermal perturbation associated with Early Devonian Intrusions in the south and unexposed sources to the east.
Volcanic troughs
- Mount Hope Trough – lower to biotite-zone greenschist contact/hydrothermal metamorphism extending into the northern deep-water basin sequences
Ural Volcanics (Rast Trough)
- Zeolite facies ocean-floor metamorphism
Deep-water Cobar Basin
- Northwestern basin – anchizone burial metamorphism
- Central basin – anchizone with zones (particularly southern central) of lower greenschist and potentially biotite-zone (e.g. Mallee Bull prospect) hydrothermal metamorphism
- Southwestern basin – immediately north of Mount Hope Trough, zone of potential pyroxene hornfels facies hydrothermal metamorphism
- Southeastern basin – immediately north of Erimeran Granite, zone of potential pyroxene hornfels facies hydrothermal metamorphism
- Northeastern basin – epizonal regional orogenic metamorphic grade, local preservation of pre-deformation biotite-zone hydrothermal metamorphism.

The most important metamorphic features for the region are:
- Basin/shelves predominantly experienced late diagenetic to anchizone burial metamorphism
- Exposed and shallowly buried I-type intrusions are confined to the southern Cobar Basin and are exclusively associated with broad zones of contact and hydrothermal metamorphism up to hornblende hornfels facies that effect both basin, volcanic tough, shelf and basement sequences.
- Epizone, hydrous greenschist facies metamorphic grades are associated with foliation development in the vicinity of interpreted basin margin and near-margin faults that accommodated significant shearing during basin inversion, particularly in the northeastern Cobar mineral field.

PETROGRAPHY OF SKARN AT HERA–NYMAGEE OREBODIES

The Hera–Nymagee orebodies are located on the eastern margin of the Cobar Basin at the boundary between the Mouramba and lower Amphitheatre groups (Figure 1). The deposits are situated on the western side of the Rookery Fault, a major orogen-parallel, near-margin basin fault (and likely pre-existing basement fault) that was reactivated during basin inversion.

The *Hera orebody* is interpreted as a single broadly stratabound orebody that has been assembled into a series of west-stepping, steeply west-dipping ore lenses (McKinnon & Fitzherbert 2017). Mineralisation occurs in vein/breccia zones predominantly hosted in intensely silicified, carbonaceous siliciclastic sequences. A halo (up to 100m) of porphyroblastic biotite is present within the siliciclastic sedimentary rocks surrounding the orebody and is locally retrogressed within a chlorite–muscovite foliation. Skarn at Hera is zoned along the strike of the orebody and mineralisation is expressed as siliciclastic-hosted veins and breccia fill, remnant

high-T skarn and sulfide phase hydrous-mineral rich skarn. In general siliciclastic host rock and clasts are intensely silicified and enveloped by sulfide-rich breccia-fill/veins, but frequently contain quartz-rich calc-silicate veins hosting garnet–zoisite–titanite–tremolite ± scheelite proximal to and within the sulfide orebody (Figure 2a, g), while a biotite-rich mineralogy dominates distal to the orebody. Garnet is absent from the north of the orebody and siliciclastic hosted calc-silicate veins and tremolite–biotite–anorthite (± scheelite) dominate the alteration assemblage here.

Remnant zones of retrograded high-T skarn/carbonate blocks/clasts within the mineralised sequence comprise garnet–diopside–quartz–zoisite–anorthite±carbonate (Figure 2b, c, d). High-T remnant skarn bodies display mineralogical zonation along the entire strike of the orebody from garnet-rich in the southern lenses (Figure 2a, b), through pyroxene-rich (+/−garnet) in the Far West lenses (Figure 2c, d) and tremolite, ±biotite, anorthite-rich (Figure 2f) (with some preserved carbonate clasts; Figure 2e) mineralogy in the North Pod.

Hydrous retrograde skarn is ubiquitous, enveloping and replacing the high-T skarn mineralogy. Hydrous skarn is sulfide-rich (sphalerite–galena–pyrrhotite±pyrite–chalcopyrite) and dominated by tremolite–biotite±garnet. Sphalerite-rich mineralisation associated with nuggetty-gold in the Far West lens is associated with a very localised calc-potassic K-feldspar–tremolite–zoisite alteration (Figure 2h). Sphalerite associated with nuggetty Au is uncharacteristically Fe-poor for the Hera orebody.

The Nearby *Nymagee orebody* (~5km North along strike from Hera) comprises three main ore lenses, with a western lode dominated by Pb–Zn sulfide and the eastern lode dominated by Cu-sulfide and lesser Fe-oxide. The gross zonation of skarn mineralogy at Nymagee is not constrained and here simply described as skarn associated with Pb–Zn–(Cu)-rich mineralisation and skarn associated with Fe-oxide, Cu-rich mineralisation. Like Hera, the Nymagee orebody is predominantly hosted within siliciclastic turbidite and localised zones of intense calc-silicate alteration. The porphyroblastic biotite halo of up to 200m within the siliciclastic rocks surrounding the Nymagee orebody is more widely developed than that around Hera. The majority of mineralisation at Nymagee is hosted within retrograde alteration zones dominated by quartz–chlorite–muscovite–illite, although quartz may be absent. Quartz–calc-silicate veins within the siliciclastic sequences are similar to the proximal veins at the Hera orebody and are dominated by garnet and tremolite, although tremolite here often pseudomorphs ex-pyroxene porphyroblasts.

Remnant high-T calc-silicate alteration comprises garnet–anorthite–zoisite–titanite–tremolite (after clinopyroxene), while sphalerite–pyrrhotite±galena commonly pseudomorph garnet. This high-T association is mostly retrogressed to talc–chlorite and illite–muscovite. Skarn associated with Fe-oxide–Cu lodes is very different and comprises aluminous Fe-rich silicates including acicular ferrotschermakite, Fe-rich biotite and epidote, which are mostly associated with the earliest Fe-oxide-rich phase of mineralisation (Figure 6c). Stilpnomelane is locally abundant, particularly in association with chalcopyrite (Figure 6d). Fe-rich chlorite and stilpnomelane are abundant as a retrograde phase throughout the ore lenses.

SELECTED MINERAL CHEMISTRY OF SKARN AT HERA–NYMAGEE OREBODIES

Mineral analyses were collected with the use of a Cameca SX-100 camebax microprobe housed at the Australian National University. The instrument was operated with an accelerating voltage of 15 kV, a beam width of 2–5 µm and data reduction software supplied by the manufacturer. All data are reported as cations per formula unit (p.f.u.).

Garnet is sub-calcic ranging from grossular to spessartine-rich compositions. Andradite contents of garnet are minimal and only values normalized to the three components $X_{grs}=Ca/(Fe + Mn + Mg + Ca)$, $X_{sps}=Mn/(Fe + Mn + Mg + Ca)$ and $X_{alm}=Fe^{2+}/(Fe^{2+} + Mn + Mg + Ca)$ are quoted below. Garnet composition is distinctly different in pelitic host rocks versus remnant carbonate-skarn. Garnet within remnant garnet–pyroxene skarn (Figure 3a) has elevated grossular component with a compositional range of X_{alm}8.29–15.85 X_{sps}23.85–41.36 X_{grs}46.23–65.76. Core to rim chemical zonation involves compositionally homogenous grossular-rich cores (host to calcite inclusions) that display sharp boundaries with rims (host to zoisite and tremolite inclusions) and grade smoothly to decreased X_{grs} and elevated X_{sps}. Garnet within siliciclastic-rock-hosted quartz–tremolite-rich veins and tremolite-rich sulfide breccia fill (Figure 3a) has elevated spessartine component varying from X_{alm}5.94–18.69 X_{sps}41.76–64.65 X_{grs}23.85–44.27 (Figure 3). Core to rim chemical zonation involves a smooth decrease in X_{sps} and sympathetic increase in X_{grs} and X_{alm} (Figure 3a). Garnet in anorthite-rich skarn from Nymagee orebody has elevated grossular and spessartine components varying from X_{alm}3.09–9.83X_{sps}35.26–49.85 X_{grs}42.03–56.79. Core to rim chemical zonation involves compositionally homogenous grossular rich cores (host to acicular ex-pyroxene inclusions) that display a sharp boundary with rims that grade smoothly to decreased X_{grs} and increased X_{sps} and elevated X_{alm} (Figure 3a) and are in equilibrium with anorthite–zoisite–tremolite rich associations.

Pyroxene from the Hera orebody is diopside (Figure 3b), although analyses display a manganoan component with Mn p.f.u ranging from 0.07 to 0.10. Pyroxene was not analysed from Nymagee orebody, although tremolite pseudomorphs after pyroxene are locally very abundant in association with garnet–anorthite skarn. Replacement by tremolite implies similar compositions to pyroxene at Hera.

Plagioclase feldspar associated with skarn from the Hera orebody is anorthite to bytwonite with An(Ca/(Ca+Na+K) = 0.83–0.96. Plagioclase feldspar from Nymagee mine is anorthite (An=0.9–1.0) and is in equilibrium with garnet. Albite was identified via XRD and is locally very abundant in association with late stage quartz bucky white quartz veins and as a late stage replacement elsewhere.

Amphibole from Hera orebody varies from actinolite to manganoan–actinolite, Si p.f.u ranges from 7.15–7.93 and X_{Mg} (Mg/Mg+Fe) ranges from 0.64–0.87 (Figure 3c). Mn is elevated, ranging from 0.12–0.48 p.f.u. Amphibole from the North Pod at Hera is exclusively tremolite, with Si p.f.u ranging from 7.49–7.82 and X_{Mg} ranging from 0.89–1.0 (Figure 3c). Amphibole

associated with retrogressed garnet–anorthite skarn from Nymagee orebody is tremolite, Si p.f.u ranging from 7.58–7.93 and XMg ranging from 0.91–1 and low Mn ranging from 0.07–0.16 p.f.u (Figure 3c). Amphibole from Fe-oxide bearing lodes at Nymagee orebody is ferrotschermakite, with Si p.f.u of 5.73–6.49 and XMg ranging from 0.16–0.32 (Figure 3c).

Epidote from Hera orebody is zoisite with $Fe^{3+}/Fe^{3+}+Al$ p.f.u ranging from 0.00–0.1596. Epidote from remnant garnet–anorthite skarn at Nymagee mine is also zoisite plotting at the low Fe end of this range. Epidote from hydrous ferrotschermakite-bearing skarn is relatively Fe-enriched with $Fe^{3+}/Fe^{3+}+Al$ p.f.u ranging from 0.20–0.25. Allanite is visible optically, particularly in the North Pod, but was not analysed as a part of this study.

STABLE ISOTOPES OF SKARN AT HERA–NYMAGEE ORE BODIES

Tremolite/actinolite from both Hera–Nymagee orebodies has a tight range of δD of −60 to −84‰ and $\delta^{18}O$ of 8 to 8.5‰, consistent with the field of magmatic waters, while biotite from the wall rocks displays lower $\delta 18O$ and higher δD, consistent with formational water input. Downes et al. (2016) describe similar trends in $\delta^{34}S$, ranging from values of ~3‰, consistent with magmatic sulfur, to values up to 10‰, consistent with formational waters.

CONCLUSIONS

The petrography and mineral chemistry described above, including sub-calcic garnet and pronounced manganoan component in garnet, pyroxene and amphibole, confirms the southeastern Cobar-type mineral deposits are unequivocally related to the retrograde phase of a strongly reduced distal skarn system. Anorthite–zoisite-rich and carbonate-poor skarn mineralogy is a reflection of low XCO2, which likely mirrors the relatively low abundance of allochthonous carbonate blocks/clasts within the mineralised stratigraphic horizon, i.e. it is a siliciclastic dominated skarn system and what little carbonate that was present has been converted to skarn. Changing skarn mineralogy within individual orebodies reflects variable thermal gradient, different host lithologies (siliciclastic versus carbonate) and hydrous recrystallisation during decreasing temperature and mineralising fluid ingress. Fe-oxide–Cu-rich lenses preserved in the Nymagee orebody represent early-formed Fe–Cu skarn that is spatially separated from Zn–Pb-rich lenses. A skarn mineral system is inconsistent with the broadly-accepted model for the formation (at least in the southeastern Cobar Basin) of Cobar-type deposits during deep burial and regional-scale ingress of basement derived fluids during basin inversion. Although no direct link to magmatic rocks has been established thus far, skarn deposits occur as very localised thermal highs punctuating a broad area of the southeastern Cobar Basin. These zones host the only exposed and shallowly buried I-type Devonian intrusions within the basin, those intrusions to the south of Hera–Nymagee (e.g. Tollingo and Fountaindale; Figure 1b), which are themselves strongly calc-potassic altered and chemically consistent with Z–Cu–W skarn formation (Blevin & Jones 2004). Changing ore mineralogy between the different orebodies (Hera and Nymagee) may be a reflection of the slightly different chemistry of driving intrusions and/or compositional variability in the host sedimentary rocks.

The known distribution of skarn mineralisation in the southeastern Cobar Basin appears to be controlled by a single (>7 km strike length) horizon that is host to shelf-derived gritstone and allochthonous carbonate blocks/clasts. Remnant high-T skarn is poorly preserved and has been recrystallised and hydrated during retrograde alteration and sulfide mineralisation. Allochthonous carbonate blocks are also present along the western margin of the basin, for example at the Norma Vale prospect, where pyroxene-rich skarn is associated with Fe(Cu)-rich mineralisation at the base of a large limestone block within the Shume Formation (Figure 1). The Shume Formation and correlative Biddabirra Formation both host allochthonous limestone and are stratigraphically higher than the Hera–Nymagee sequences, suggesting there are a number of prospective allochthonous packages within the Cobar Basin stratigraphy. The lower Cobar Basin sequences comprises shallow water reef to shelf sequences developed at the early stage of rifting. These lower basin sequences also host abundant conglomerate and carbonate, and with a shift in paradigm to a skarn mineral system model these shelf sequences also become highly prospective. The deeper-water Cobar Basin is also flanked to the west and east by carbonate and volcanic shelf sequences. Although the western carbonate shelf (Winduck Shelf) appears to be more closely associated with cooler Mississippi Valley style mineralisation, the eastern shelf (Kopyje Shelf) is host to limestone and a number syn-rift intrusive/volcanic rocks, and is highly prospective for skarn mineralisation. Zn skarn akin to the Hera-Nymagee orebodies generally occurs in the distal portions of major magmatic/hydrothermal systems, summed up by Magaw et al. (1988), who noted that many Zn skarn districts grade outward from intrusion associated mineralisation to intrusion free ores, which suggests that those districts lacking known intrusive relationships may not have been traced to their ends, implying that as a newly defined distal (intrusion distal) skarn district, the southern Cobar Basin is immature with respect to exploration for skarn and proximal intrusion-related mineral systems.

ACKNOWLEDGMENTS

REFERENCES

Berthelsen R. 2010. Cobar goldfield mineral deposits. Abstracts; Giant ore deposits down-under, 13th Quadrennial IAGOD symposium, Adelaide, Australia.

Blevin P.L & Jones M. 2004. Chemistry, age and metallogeny of the granites and related rocks of the Nymagee region, NSW. In: McQueen K.G. & Scott K.M. eds. Proceedings of the Exploration Field Workshop, Cobar Region, 2004, pp. 15–19, CRC LEME Publication.

Brown B., Ashley P., Vickery N., Tyson R. & Oates M. 2015. Significant recent developments and research at the Mallee Bull deposit, Cobar Basin, NSW. In: P.C. Lewis ed. 2015, Australian Institute of Geoscientists Bulletin 62.

Cleverley J.S. and Barnicoat A.C. 2007. Fluids, sources and reservoirs. In: van der Wielen. S. & Korsch. R. eds. 2007. 3D Architecture and Predictive Mineral System Analysis of the Central Lachlan Subprovince and Cobar Basin, New South Wales, pp 117–121. Final Report for the pmd*CRC T11 project. Geoscience Australia, Canberra.

David V. 2006. Cobar Superbasin System metallogenesis. In: Lewis P.C. ed. Mineral Exploration Geoscience in New South Wales, Extended Abstracts, pp. 39–51. Mines and Wines Conference 2006, Cessnock NSW, SMEDG (Sydney Mineral Exploration Discussion Group).

Downes P. M., Blevin P., Armstrong R., Simpson C.J., Sherwin L., Tilley D.B. & Burton G.R. 2016. Outcomes of the Nymagee mineral system study — an improved understanding of the timing of events and prospectivity of the Central Lachlan Orogen. Quarterly Notes of the Geological Survey of New South Wales 147.

Fitzherbert J.A., Downes P.M., and Blevin P.L. 2016. Cobar Special 1:500 000 Metallogenic Map. Geological Survey of New South Wales, Maitland, Australia.

Fitzherbert J.A., Mawson R., Mathieson D., Simpson A.J., Simpson C.J., and Nelson M.J. 2017a. Metamorphism in the Cobar Basin: Current state of understanding and implications for mineralisation. Quarterly Notes of the Geological Survey of New South Wales 148.

Fitzherbert J.A., Blevin, P.L., McKinnon, A.R. 2017b. Turbidite-hosted intrusion-related mineralisation in the eastern Cobar Basin: new insights from the south. Discoveries in the Tasmanides, conference abstracts.

Glen R.A., Clare, A. and Spencer, R. 1996. Extrapolating the Cobar Basin model to the regional scale: Devonian basin-formation and inversion in western New South Wales. In: Cook W. G., Ford A. J. H., McDermott J. J., Standish P. N., Stegman C. L. & Stegman T. M. eds. The Cobar Mineral Field – A 1996 Perspective, pp.43–83. Australasian Institute of Mining and Metallurgy, Melbourne, 3/96.

Glen R.A., Dallmeyer R.D., and Black L.P. 1992. Isotopic dating of basin inversion — the Palaeozoic Cobar Basin, Lachlan Orogen, Australia. Tectonophysics 214, 249–268.

Lawrie K.C. & Hinman M.C. 1998. Cobar-style polymetallic Au–Cu–Ag–Pb–Zn deposits. AGSO Journal of Australian Geology and Geophysics 17(4), 169–187.

Leake B., Woolley A.A., Arps. C.E.S., Birch W.D., Gilbert M.C., Grice J.D., Hawthorne F.C., Kato A., Kisch H.J., KrlVovichev V.G., Linthout K., Laird J., and Mandarino J. 1997. Nomenclature of Amphiboles: Report of the Subcommittee on Amphiboles of the International Mineralogical Association Commission on New Minerals and Mineral Names. Mineralogical Magazine 61, 295–321.

Mackinnon A.R., & Fitzherbert, J.A., 2017. New developments at the Hera Au–Pb–Zn–Ag Mine, Nymagee, New South Wales, Discoveries in the Tasmanides, conference abstracts.

Megaw, P., Ruiz, J., and Titley, S., 1988, High temperature, carbonate-hosted Ag–Pb–Zn(Cu) deposits of northern Mexico: Economic Geology and the Bulletin of the Society of Economic Geologists, v. 83, p. 1856–1885.

Stegman C. L. 2001. Cobar deposits: still defining classification. Society of Economic Geologists Newsletter 44, 15–25.

Suppel, D.W. 1984. A study of mineral deposits in the Cobar Supergroup, Cobar region, New South Wales. MSc thesis, University of New South Wales, Sydney (unpubl.).
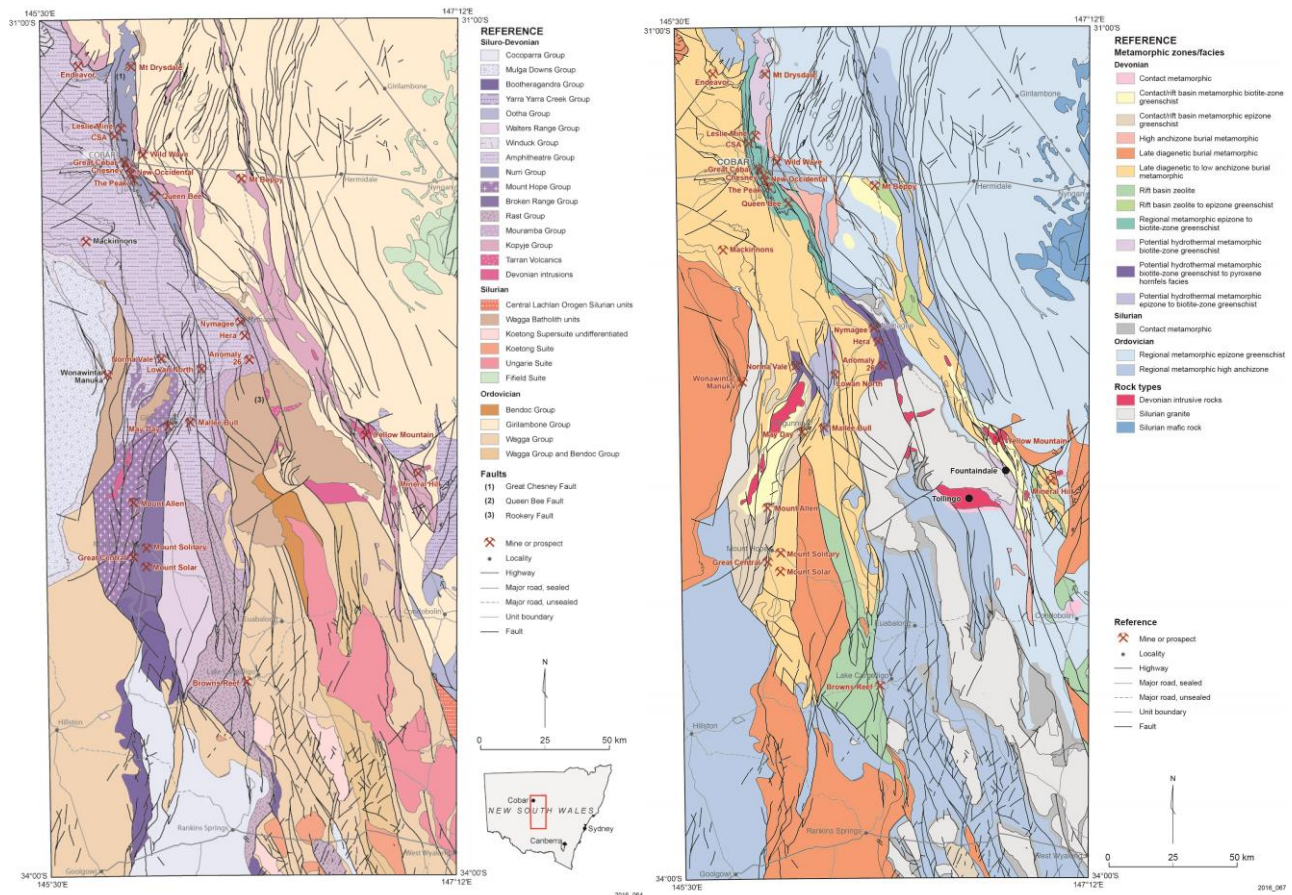
Figure 1a) Group level distribution of the Cobar Basin and basement with a selection of important mineral deposits/prospects (after Fitzherbert et al. 2017). Undercover interpretation based on Fitzherbert et al. 2016, **b)** Metamorphic map of the Cobar Basin after Fitzherbert et al. (2017) with mineral deposits/prospects referred to in the text. Devonian intrusive rocks are highlighted in red.
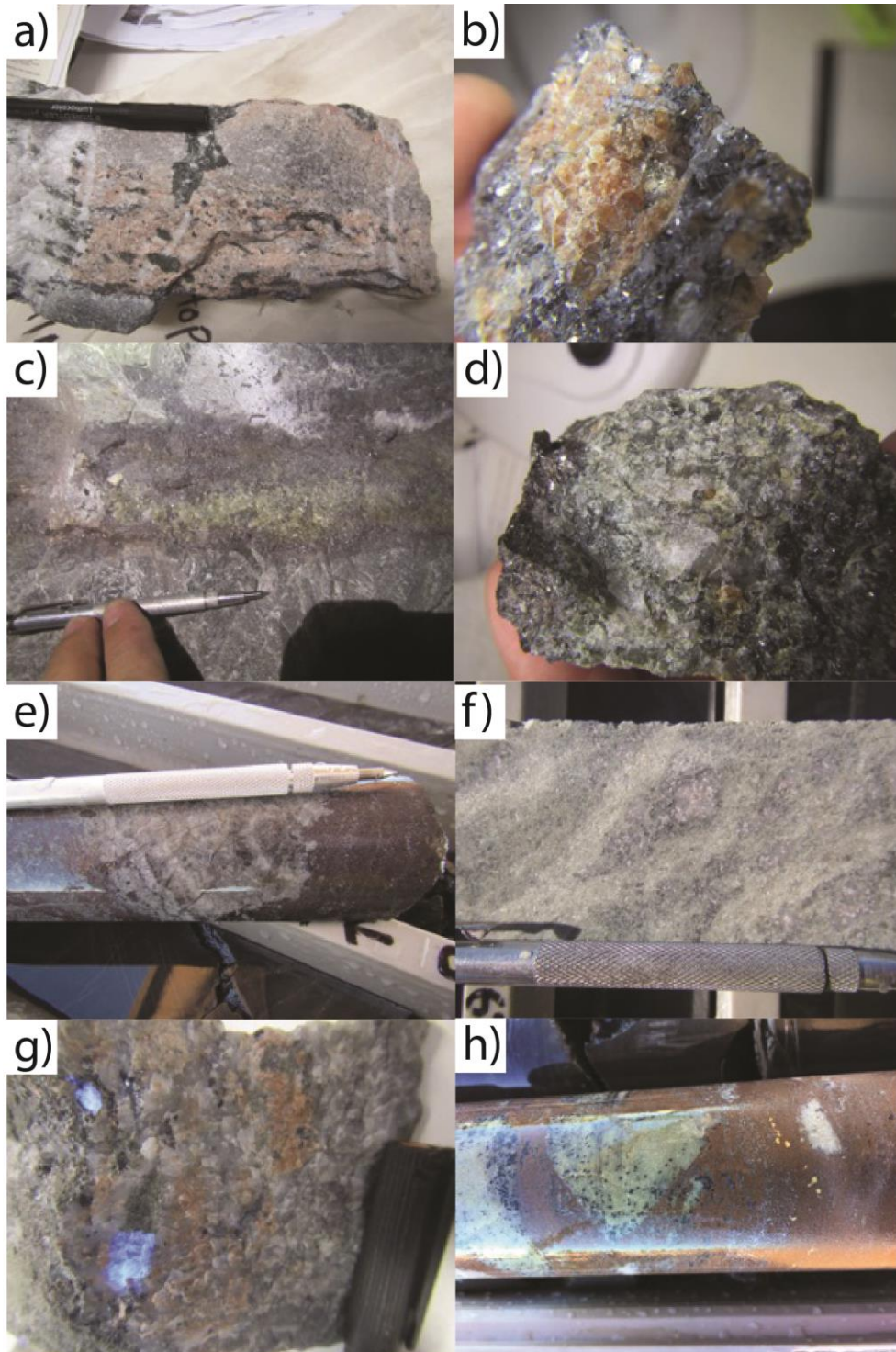
Figure 2a) Garnet-flooded sandstone horizon from southern Hera orebody. b) Garnet-rich skarn clast within massive sulfide from southern Hera orebody (Main North Lode), c) pyroxene skarn enveloped by massive sulfide from central Hera orebody (Far West Lode), d) pyroxene–garnet skarn from central Hera orebody (Far West Lode), e) remnant laminated dolomite clast enveloped by massive sulfide from northern Hera orebody (North Pod), f) anorthite–tremolite skarn from northern Hera orebody, g) quartz–garnet–scheelite vein from southern-central Hera orebody (low moly scheelite, blue fluorescence under short wavelength UV light), h) nuggetty gold associated with low-Fe sphalerite (brown) and clasts of skarn altered (tremolite–anorthite–K-feldpsar) siltstone.
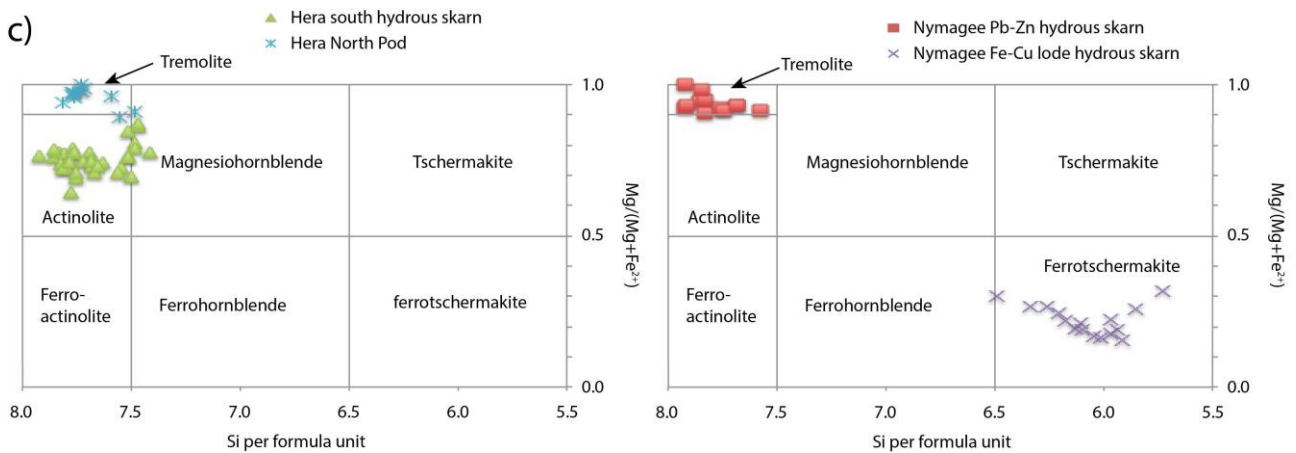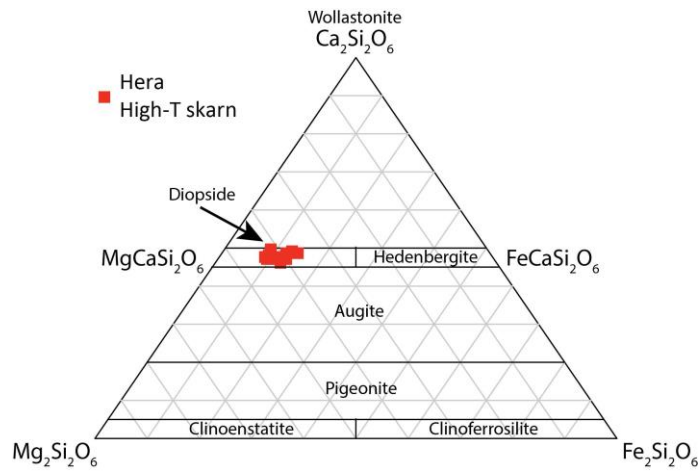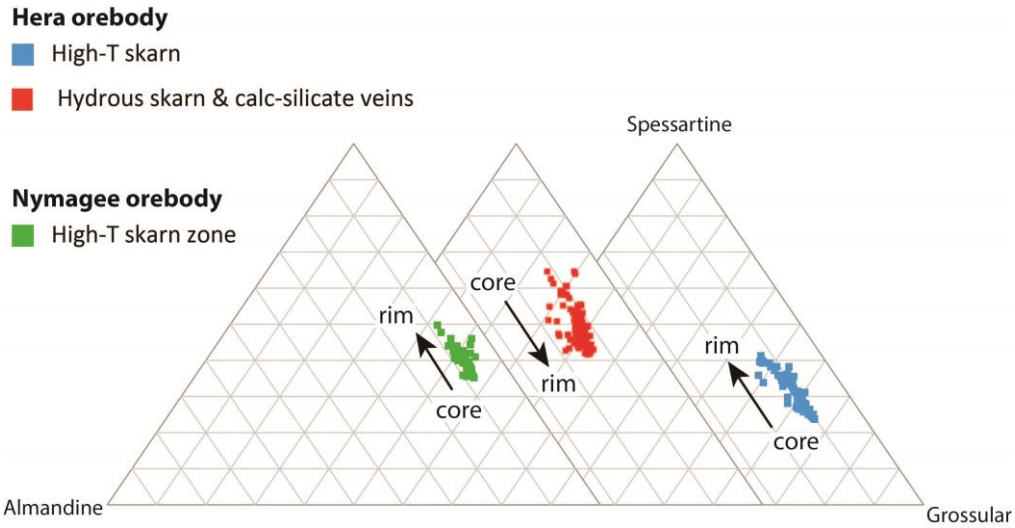
Figure 3a) Ternary plots of skarn garnet compostion from Hera and Nymagee orebodies. General core to rim compositional trends of single garnet grains are indicated by arrows (see text for end-member compositional information). b) Ternary plot of pyroxene compostion from Hera orebody (see text for details). Classification of amphiboles from Hera and Nymagee orebodies based on Leeke (1997).